nature geoscience

ARTICLES

https://doi.org/10.1038/s41561-020-0602-5

Check for updates

Mud in rivers transported as flocculated and suspended bed material

Michael P. Lamb[1]✉, Jan de Leeuw[1], Woodward W. Fischer[1], Andrew J. Moodie[2], Jeremy G. Venditti[3,4], Jeffrey A. Nittrouer[2], Daniel Haught[3] and Gary Parker[5,6]

Riverine transport of silt and clay particles—or mud—builds continental landscapes and dominates the fluxes of sediment and organic carbon across Earth's surface. Compared with fluxes of sand-sized grains, mud fluxes are difficult to predict. Yet, understanding the fate of muddy river sediment is fundamental to the global carbon cycle, coastal landscape resilience to sea-level rise, river restoration and river–floodplain morphodynamics on Earth and Mars. Mechanistic theories exist for suspended sand transport, but mud in rivers is often thought to constitute washload—sediment with settling velocities so slow that it does not interact with the bed, such that it depends only on upstream supply and is impossible to predict from local hydraulics. To test this hypothesis, we compiled sediment concentration profiles from the literature from eight rivers and used an inversion technique to determine settling rates of suspended mud. We found that mud in rivers is largely flocculated in aggregates that have near-constant settling velocities, independent of grain size, of approximately 0.34 mm s^{-1}, which is 100-fold faster than rates for individual particles. Our findings indicate that flocculated mud is part of suspended bed-material load, not washload, and thus can be physically described by bed-material entrainment theory.

Mud has long been thought to constitute the washload—the portion of river sediment loads that settles too slowly to actively interchange with or be sourced from the sediment bed[1,2]. Unlike the coarser bed-material load that can be predicted from entrainment relations that depend on particle size and bed fluid stresses[3], washload flux is governed by sediment supply from upstream[1,4]. Consequently, mud transport is thought to depend on catchment geology, climate-influenced weathering rates and physical weathering processes in uplands such as landsliding, all of which are difficult to constrain[5]. Thus, in the absence of a universal theory, mud transport must be measured directly, which is hard to do for all rivers at all times[6].

Although mud is often assumed to be washload either by definition[1] or by its low abundance in the riverbed (<10% by mass[2], for example), observations suggest that mud does interact and interchange with the bed sediment. For example, a 2 µm clay particle has such a small settling velocity that it should be transported ~1,500 km downstream before it settles through a 5 m water column, given a typical river velocity of 1 m s^{-1}. This extreme transport distance, however, is inconsistent with geochemical tracer observations that show mud has transport lengths ~100-fold shorter[7]. Even on floodplains with slower and shallower flows, settling clay should be dispersed tens of kilometres from river channels. However, observations show that lowland rivers are bounded by levees actively built by overbank flows—many of these are composed of mud, some with high clay contents (for example, ~50%; ref. [8]). Moreover, deposition rates on alluvial ridges decline exponentially away from the channel and imply transport lengths of tens to hundreds of metres[9,10], not tens of kilometres.

We investigated the hypothesis that mud transport can be predicted from relations for suspended bed-material load based on evidence that mud is flocculated and thus has considerably greater settling velocities than are typically assumed[11]. Flocculation is the processes by which particles aggregate to form composite structures, referred to as flocs[12]. It is well accepted that flocculation controls transport and depositional patterns of mud in estuaries and marine environments[13], where saline water neutralizes mineral surface charges and reduces repulsion between particles[14] and where organic matter can help bind particles into aggegates[15,16]. However, flocculation is generally assumed to be negligible in freshwater rivers, and it is not included in models of river sediment transport and fluvial morphodynamics[1,10]. Nonetheless, flocs have been observed in some freshwater rivers in association with organic matter[17,18].

Suspended sediment concentration profiles

We evaluated flocculation in rivers using a global compilation of 180 sediment concentration profiles from 8 lowland, sand-bedded rivers (Methods). If flocculation is important, it should affect the reach-scale sediment transport dynamics of rivers, which would be reflected in the vertical concentration profiles of the mud fraction[19]. Furthermore, we tested whether or not suspended mud is part of the suspended bed-material load (rather than washload) by comparing near-bed mud concentrations to theory for equilibrium bed-material entrainment[20], while accounting for flocculation and the small percentage of mud that exists in the beds of rivers.

Vertical concentration profiles of suspended sediment in rivers are set by a balance between an upward flux of sediment due to turbulent mixing and a downward flux due to particle settling; this is represented at equilibrium by Rouse theory[19], written here for a mixture of particle sizes,

[1]Division of Geological and Planetary Sciences, California Institute of Technology, Pasadena, CA, USA. [2]Department of Earth, Environmental and Planetary Sciences, Rice University, Houston, TX, USA. [3]Department of Geography, Simon Fraser University, Burnaby, British Columbia, Canada. [4]School of Environmental Science, Simon Fraser University, Burnaby, British Columbia, Canada. [5]Ven Te Chow Hydrosystems Laboratory, Department of Civil and Environmental Engineering, University of Illinois at Urbana-Champaign, Champaign, IL, USA. [6]Department of Geology, University of Illinois at Urbana-Champaign, Champaign, IL, USA. ✉e-mail: mpl@gps.caltech.edu

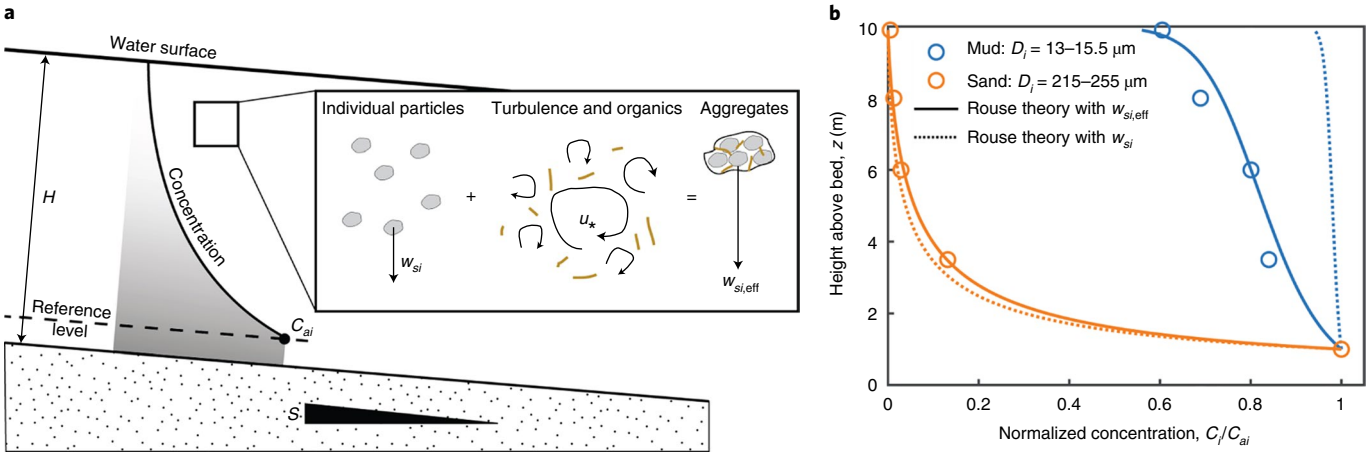

Fig. 1 | Sediment suspension profiles. a, Schematic cross-section of H and bed slope S showing a concentration profile governed by w_{si} and u_*. Flocculation increases $w_{si,eff}$, resulting in a greater concentration gradient with depth. **b**, Example grain-size-specific vertical concentration profiles from the Ganges River[38] showing that sand follows Rouse theory (equation (1)), whereas the mud fraction deviates substantially from theory when using w_{si}. The best-fit Rouse number was used to find $w_{si,eff}$.

$$\frac{C_i}{C_{ai}} = \left[\frac{(H-z)/z}{(H-a)/a}\right]^{P_i} \quad (1)$$

where C_i is the volumetric sediment concentration of a given (ith) grain-size class at elevation z above the bed, C_{ai} is the grain-size-specific near-bed reference concentration at $z=a$, and H is the flow depth. P_i denotes the Rouse number for grain-size class i:

$$P_i = \frac{w_{si,\mathrm{eff}}}{\beta_i \kappa u_{*\mathrm{sk}}} \quad (2)$$

in which $w_{si,\mathrm{eff}}$ is the effective particle settling velocity, $\kappa = 0.41$ is von Karman's constant, $u_{*\mathrm{sk}}$ is the skin-friction portion of the bed shear velocity (Methods)—used here rather than total shear velocity based on the finding of Leeuw et al.[20]—and β_i is a factor that accounts for differences in the fluid turbulence and sediment diffusivities, and turbulence damping due to stratification (Methods). Individual mud particles have such small settling velocities that $P_i \ll 1$ (equation (2)), and therefore concentration profiles with depth should be constant (that is, $C_i(z) = C_{ai}$; Fig. 1a). If mud is flocculated, however, $w_{si,\mathrm{eff}}$ will be larger than the theoretical settling velocity for individual particles, w_{si}, causing a vertical gradient in the concentration profiles of mud (Fig. 1a). Suspended sediment stratification can also can cause concentration profiles to deviate from Rouse theory due to the suppression of turbulent mixing[3]; however, turbulence damping should affect concentration profiles of all particle sizes by modifying $u_{*\mathrm{sk}}$ or β_i, whereas flocculation should affect only the finest fractions by modifying $w_{si,\mathrm{eff}}$. Thus, the grain-size specific vertical concentration profiles from rivers can be used to calculate $w_{si,\mathrm{eff}}$ from equations (1) and (2) and to determine whether mud in rivers is flocculated.

We compiled sediment-size-specific concentration profiles, bed grain-size distributions and all other parameters needed to constrain equations (1) and (2) (Methods). We analysed the mud fractions (grain diameters, $D_i < 62.5\,\mu\mathrm{m}$)—these typically constituted more than 80% of the suspended sediment in the water column, and only a small fraction (typically <15%) of the bed material (Extended Data Fig. 1). The concentration profile for each grain-size class was fit to equation (1) using least-squares regression applied to the logarithm of the data to find P_i, and then the effective settling velocity was calculated from equation (2) (Methods). We also found the best-fit near-bed concentration for each grain-size class, and compared this to an empirical theory for the entrainment of bed material into suspension (Methods). The theory predicts near-bed concentration as a function of bed stress and the fraction of each grain-size class in the riverbed, and fits the sand data from the same dataset well[20].

Enhanced in situ settling velocities of mud particles

The results show substantial differences between the concentration–depth profiles for mud particles predicted by theory and those actually observed in rivers (Fig. 1b). While the sand fractions had profiles that agree with Rouse theory, the mud fractions were not homogeneously mixed as theory predicts. Rouse numbers for the sand and coarse silt follow a power-law trend with $u_{*\mathrm{sk}}/w_{si}$ (Fig. 2a), as expected by Rouse theory (equation (2)), and the relation improves when the dependence of β_i on flow resistance, C_f, is included (Fig. 2b) (Methods). Likewise, effective settling velocities of coarse silt and sand ($D_i > 40\,\mu\mathrm{m}$), calculated from best-fit Rouse numbers, increase with the square of particle diameter, following theory for the settling of individual particles (Fig. 2c). However, the mud data deviate substantially from Rouse theory; they exhibit little trend with $u_{*\mathrm{sk}}/w_{si}$ (Fig. 2b), suggesting that the mud was flocculated. Moreover, mud particles have near-uniform effective settling velocities with a geometric mean of 0.34 mm s^{-1} (range: 0.17–0.70 mm s^{-1}, representing one geometric s.d.)—rates that are up to 400 times larger than those expected for the settling of isolated particles (Fig. 2c), but are similar to floc settling velocities observed in estuarine and marine environments (~1 mm s^{-1}; ref. [13]).

We interpret the near-uniform settling rates (Fig. 2c) and the deviation from Rouse theory (Fig. 2a,b) of particles $D_i < 40\,\mu\mathrm{m}$ as indications that these particles were flocculated—exhibiting much greater settling velocities than expected for their individual particle sizes. The sizes and densities of flocs were inferred from a model for floc formation[21] (Methods), which relates the effective floc diameter, D_f, to its submerged specific density: $R_f = R_p(D_f/D_p)^{n_f-3}$ where D_p and R_p are the constituent particle median diameter and submerged specific density, respectively, and the fractal dimension is typically $n_f = 2.5$. In combination with a settling velocity model[22,23] (Methods), we calculated that the freshwater flocs had diameters of 150–250 μm (similar to fine sand), but with settling velocities equivalent to ~20 μm silt because of their low submerged densities ($R_f \approx 0.5$) (Fig. 3).

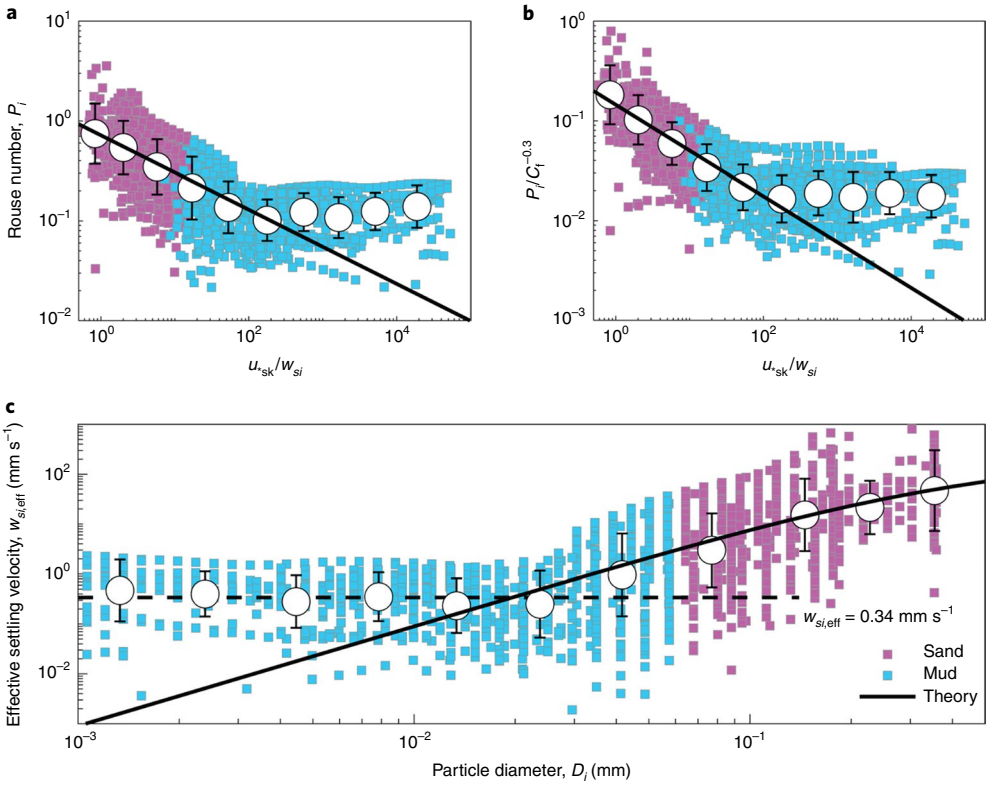

Fig. 2 | Mud transport data compared to theory. a, Best-fit Rouse parameters, P_i, from suspension profiles versus u_{*sk}, normalized by w_{si}, showing systematic deviation of the mud fraction from a one-parameter model for sand[20] with $\beta_i = 3.4\left(\frac{u_{*sk}}{w_{si}}\right)^{-0.63}$ (Methods). Each square represents a grain-size specific concentration profile, and larger circles are binned geometric means ± 1 s.d. (error bars). **b**, Same as **a** but Rouse parameters were normalized to account for the secondary dependence of β_i on C_f in the two-parameter model for sand[20] with $\beta_i = 16.82\left(\frac{u_{*sk}}{w_{si}}\right)^{-0.54} C_f^{0.3}$ (Methods). **c**, Effective settling velocities derived from concentration profiles as a function of particle diameter, showing that the mud fraction systematically deviates from theory[39] (black line) for settling of individual particles (Methods). The legend in **c** applies to all panels.

Our results are consistent with individual observations of freshwater flocs in this size range using in situ laser diffraction or microscopic analyses of filtered particles[17,24]. Freshwater flocs have been observed to be bound by polymeric organic material and often colonized by microorganisms[25] forming composite structures of inorganic and organic particles, microbial communities and pore spaces[12]. Some riverine flocs may form as soil aggregates; however, experiments indicate that soil aggregates break up in rivers due to turbulence, and then reform in equilibrium with fluvial conditions[26,27]. Experiments also have shown that freshwater flocs readily form in the presence of some idealized terrestrial organic polymeric substances[28,29].

The range in observed effective settling velocities for mud is surprisingly small given that the data include different rivers with different shear stresses, sediment-size distributions and catchments with different geology and climates (Extended Data Table 1). Some of these variables are known to affect flocculation dynamics and might explain the observed variability in $w_{si,eff}$ (refs. [22,23]). In addition, the variability in effective settling velocities for mud is similar to that observed for sand (Fig. 2c), suggesting that the variability might result from processes not captured in our model. For example, particle shape alone can account for a factor of ten in settling rates in the absence of flocculation[30]. And as the Rouse model (equation (1)) is a one-dimensional approximation of suspension dynamics, there also is variability in the concentration–depth profile data that underlie the best-fit model used to calculate effective settling velocity (Fig. 2b,c). Despite this variation, the enhanced settling rates for mud when compared to the theory for individual particles is substantial and systematic across the wide range of rivers analysed. Flocculation in rivers might be ubiquitous.

Flocculated mud as suspended bed-material load

The large effective settling velocities we observed for mud imply that these particles might not be the supply-limited passive tracers assumed in the washload paradigm, but instead can settle to, and be resuspended from, the riverbed. If correct, mud can be predicted from bed entrainment theory[31]. To test this idea, we compared the grain-size-specific near-bed concentrations of mud to empirical theory for equilibrium near-bed concentrations of bed-material transport that were derived from the sand fractions in our dataset[20]:

$$C_{ai} = Af_i(u_{*sk}/w_{si})^a \mathrm{Fr}^b \quad (3)$$

where f_i is the volume fraction of a certain grain-size class in the bed sediment, Fr is the Froude number (Methods) and $A = 4.74 \times 10^{-4}$, $a = 1.77$ and $b = 1.18$ are empirical constants. To account for flocculation, we summed the bed fractions and near-bed concentrations for $D_i < 40\,\mu$m, and used the effective settling velocities we inferred for flocs, rather than settling velocities expected of individual particles. Accounting for flocculation, the theory for equilibrium bed-material transport can explain the observed concentrations of suspended mud as well as coarser silt and sand (Fig. 4). In contrast, without flocculation, individual mud particles are predicted to have concentrations up to five orders of magnitude larger than observed, and in many cases they surpass the theoretical limit of 100% solids by volume (Fig. 4). This analysis suggests that flocculated mud is

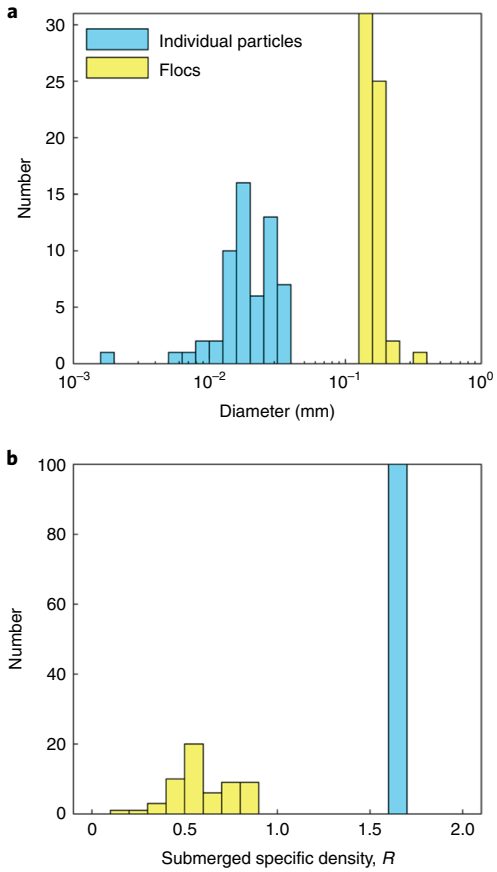

Fig. 3 | Floc properties. a,**b**, Median particle diameters (**a**) and submerged specific density (**b**) based on the size distribution of measured individual particles that are inferred to compose flocs ($D_i < 40\,\mu m$), and calculations for floc diameter and floc submerged specific density for aggregated particles using floc formation and settling models[21–23] (Methods).

part of the suspended bed-material load, not washload, and can be predicted with knowledge of the local hydraulics that entrain mud from the bed.

Mud dominates the suspended load of rivers while typically constituting a small fraction of the bed sediment (Extended Data Fig. 1); this has been used previously to infer that mud must be sourced from upstream and transported as washload[2]. In contrast, our analyses suggest that suspended mud in the water column is in dynamic equilibrium with the riverbed material through f_i (equation (3)). Despite small f_i, mud dominates the suspended load because of high entrainment rates driven by large u_{*sk}/w_{si}. Although individual flocs probably do not persist intact through cycles of deposition and entrainment, flocs may rapidly reform and thereby control mud settling rates despite active bed interchange.

Greater settling velocities of mud due to flocculation help explain observations of relatively short transport lengths—this has implications for the residence time of pollutants[7,32], coastal landscape resilience to sea-level rise[33] and the ability of floodplain storage to buffer changes in the carbon cycle[34]. The interaction of flocculated mud with the riverbed also can contribute to morphodynamic feedbacks between topography, hydraulics and sediment transport that drive landform evolution. For example, flocculation can explain mud deposition rates over tens to hundreds of metres on river levees, the lack of cross-stream fining of overbank floodplain deposits and clay in channel-proximal deposits[8,32]. Channel-proximal deposits of mud may, in turn, control river bank strength, bank erosion rates[35] and river channel geometries such as the onset of meandering[36].

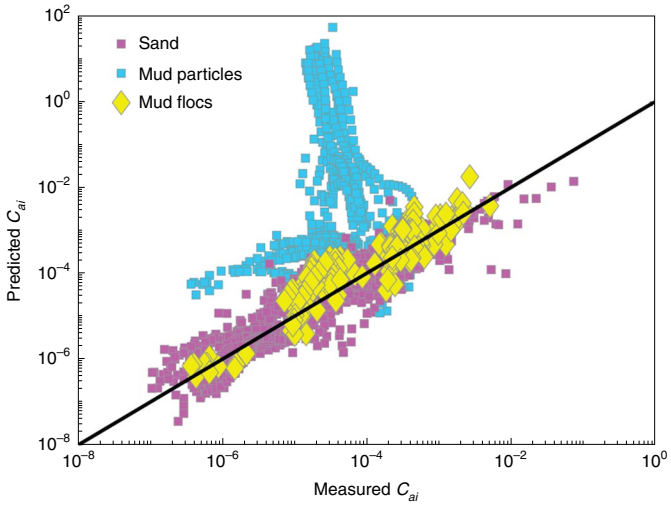

Fig. 4 | Suspended bed-material entrainment. Measured near-bed (10% flow depth) grain-size-specific concentration data for sand and mud evaluated as individual particles, and the same mud data evaluated as flocculated aggregates, compared to theory for entrainment of bed material into suspension (black line[25]; see equation (3) and Methods). Transported sediment that matches theory is considered suspended bed-material load, whereas washload is not expected to match.

Mud dominates the sediment load of rivers worldwide and the delivery of organic carbon to sedimentary basins[5,37]. If mud is part of the suspended bed-material load in rivers, as indicated by our results, then mud and carbon fluxes depend on measurable local grain-size distributions and flow hydraulics, rather than on the complex, idiosyncratic weathering and hillslope processes considered under the washload paradigm.

Online content

Any methods, additional references, Nature Research reporting summaries, source data, extended data, supplementary information, acknowledgements, peer review information; details of author contributions and competing interests; and statements of data and code availability are available at https://doi.org/10.1038/s41561-020-0602-5.

Received: 11 December 2019; Accepted: 22 May 2020;
Published online: 06 July 2020

References

1. Parker, G. *1D Sediment Transport Morphodynamics With Applications to Rivers and Turbidity Currents* http://hydrolab.illinois.edu/people/parkerg/powerpoint_lectures.htm (2009).
2. Church, M. Bed material transport and the morhology of alluvial river channels. *Annu. Rev. Earth Planet. Sci.* **34**, 325–354 (2006).
3. Wright, S. & Parker, G. Flow resistance and suspended load in sand-bed rivers: simplified stratification model. *J. Hydraul. Eng.* **130**, 796–805 (2004).
4. Einstein, H. A. & Johnson, J. W. in *Applied Sedimentation* (ed. Trask, P. D.) 62–71 (John Wiley & Sons, 1950).
5. Syvitski, J. P. M. & Milliman, J. D. Geology, geography, and humans battle for dominance over the delivery of fluvial sediment to the coastal ocean. *J. Geol.* **115**, 1–19 (2007).
6. Wang, J. et al. Controls on fluvial evacuation of sediment from earthquake-triggered landslides. *Geology* **43**, 115–118 (2015).
7. Pizzuto, J. E. Long-term storage and transport length scale of fine sediment: analysis of a mercury release into a river. *Geophys. Res. Lett.* **41**, 5875–5882 (2014).
8. Aalto, R., Lauer, J. W. & Dietrich, W. E. Spatial and temporal dynamics of sediment accumulation and exchange along Strickland River floodplains (Papua New Guinea) over decadal-to-centennial timescales. *J. Geophys. Res. Earth Surf.* **113**, F01S04 (2008).

9. Adams, P. N., Slingerland, R. L. & Smith, N. D. Variations in natural levee morphology in anastomosed channel flood plain complexes. *Geomorphology* **61**, 127–142 (2004).
10. Hajek, E. A. & Wolinsky, M. A. Simplified process modeling of river avulsion and alluvial architecture: connecting models and field data. *Sediment. Geol.* **257-260**, 1–30 (2012).
11. Bouchez, J. et al. Prediction of depth-integrated fluxes of suspended sediment in the Amazon River: particle aggregation as a complicating factor. *Hydrol. Process.* **25**, 778–794 (2011).
12. Droppo, I. G. Rethinking what constitutes suspended sediment. *Hydrol. Process.* **15**, 1551–1564 (2001).
13. Hill, P. S., Milligan, T. G. & Geyer, W. R. Controls on effective settling velocity of suspended sediment in the Eel River flood plume. *Cont. Shelf Res.* **20**, 2095–2111 (2000).
14. Sutherland, B. R., Barrett, K. J. & Gingras, M. K. Clay settling in fresh and salt water. *Environ. Fluid Mech.* **15**, 147–160 (2014).
15. Dyer, K. R. Sediment processes in estuaries: future research requirements. *J. Geophys. Res.* **94**, 14327 (1989).
16. Winterwerp, J. C. On the flocculation and settling velocity of estuarine mud. *Cont. Shelf Res.* **22**, 1339–1360 (2002).
17. Nicholas, A. P. & Walling, D. E. The significance of particle aggregation in the overbank deposition of suspended sediment on river floodplains. *J. Hydrol.* **186**, 275–293 (1996).
18. Bungartz, H. & Wanner, S. C. Significance of particle interaction to the modelling of cohesive sediment transport in rivers. *Hydrol. Process.* **18**, 1685–1702 (2004).
19. Rouse, H. R. Modern conceptions of the mechanics of turbulence. *Trans. Am. Soc. Civ. Eng.* **102**, 463–543 (1937).
20. de Leeuw, J. et al. Entrainment and suspension of sand and gravel. *Earth Surf. Dynam.* **8**, 485–504 (2020).
21. Kranenburg, C. The fractal structure of cohesive sediment aggregates. *Estuar. Coast. Shelf Sci.* **39**, 451–460 (1994).
22. Winterwerp, J. C. A simple model for turbulence induced flocculation of cohesive sediment. *J. Hydraul. Eng.* **36**, 309–326 (1998).
23. Strom, K. & Keyvani, A. An explicit full-range settling velocity equation for mud flocs. *J. Sediment. Res.* **81**, 921–934 (2011).
24. Wendling, V. et al. Using an optical settling column to assess suspension characteristics within the free, flocculation, and hindered settling regimes. *J. Soils Sediments* **15**, 1991–2003 (2015).
25. Beckett, R. & Le, N. P. The role of organic matter and ionic composition in determining the surface charge of suspended particle in natural waters. *Colloids Surf.* **44**, 35–49 (1990).
26. Grangeon, T., Droppo, I. G., Legout, C. & Esteves, M. From soil aggregates to riverine flocs: a laboratory experiment assessing the respective effects of soil type and flow shear stress on particles characteristics. *Hydrol. Process.* **28**, 4141–4155 (2014).
27. Wendling, V., Legout, C., Gratiot, N., Michallet, H. & Grangeon, T. Dynamics of soil aggregate size in turbulent flow: respective effect of soil type and suspended concentration. *CATENA* **141**, 66–72 (2016).
28. Tang, F. H. M. & Maggi, F. A mesocosm experiment of suspended particulate matter dynamics in nutrient- and biomass-affected waters. *Water Res.* **89**, 76–86 (2016).
29. Furukawa, Y., Reed, A. H. & Zhang, G. Effect of organic matter on estuarine flocculation: a laboratory study using montmorillonite, humic acid, xanthan gum, guar gum and natural estuarine flocs. *Geochem. Trans.* **15**, 1 (2014).
30. Dietrich, W. E. Settling velocity of natural particles. *Water Resour. Res.* **18**, 1615–1626 (1982).
31. Einstein, H. A. & Chien, N. Can the rate of wash load be predicted from the bed-load function? *Trans. Am. Geophys. Union* **34**, 876–882 (1953).
32. He, Q. & Walling, D. E. Spatial variability of the particle size composition of overbank floodplain deposits. *Water Air Soil Pollut.* **99**, 71–80 (1997).
33. Edmonds, D. A. & Slingerland, R. L. Significant effect of sediment cohesion on delta morphology. *Nat. Geosci.* **3**, 105–109 (2010).
34. Torres, M. A. et al. Model predictions of long-lived storage of organic carbon in river deposits. *Earth Surf. Dynam.* **5**, 711–730 (2017).
35. Lapôtre, M. G. A., Ielpi, A., Lamb, M. P., Williams, R. M. E. & Knoll, A. H. Model for the formation of single-thread rivers in barren landscapes and implications for pre-Silurian and Martian fluvial deposits. *J. Geophys. Res. Earth Surf.* **124**, 2757–2777 (2019).
36. Peakall, J., Ashworth, P. J. & Best, J. L. Meander-bend evolution, alluvial architecture, and the role of cohesion in sinuous river channels: a flume study. *J. Sediment. Res.* **77**, 197–212 (2007).
37. Leithold, E. L., Blair, N. E. & Wegmann, K. W. Source-to-sink sedimentary systems and global carbon burial: a river runs through it. *Earth Sci. Rev.* **153**, 30–42 (2016).
38. Lupker, M. et al. A Rouse-based method to integrate the chemical composition of river sediments: application to the Ganga basin. *J. Geophys. Res. Earth Surf.* **116**, F04012 (2011).
39. Ferguson, R. I. & Church, M. A simple universal equation for grain settling velocity. *J. Sediment. Res.* **74**, 933–937 (2004).

Publisher's note Springer Nature remains neutral with regard to jurisdictional claims in published maps and institutional affiliations.

© The Author(s), under exclusive licence to Springer Nature Limited 2020

Methods

Our database contains 180 concentration profiles from 8 rivers and 62 profiles from 6 different experimental studies (Extended Data Table 1), although only the data from natural rivers that contained mud were analysed herein[38,40–46]. This is an exhaustive compilation of studies that reported suspended sediment profiles $C(z)$, depth-averaged flow velocity (U), H, S and the grain-size distribution of the bed material and the suspended sediment samples. The Froude number was calculated as $\mathrm{Fr} = \mathrm{U}/\sqrt{\mathrm{gH}}$, in which g is the acceleration due to gravity. The sand data ($D_i > 62.5\,\mu\mathrm{m}$) was analysed in de Leeuw et al.[20] and we followed the same approach for mud.

Vertical concentration profiles were discretized into grain-size specific classes as $C_i = f_i C_{\mathrm{tot}}$, where C_{tot} is the total suspended sediment concentration for all sizes. For each grain-size-specific profile, we fit the Rouse formula (equation (1)) in log-transformed space using linear least squares to find the best-fit Rouse number, and then calculated the effective settling velocity from equation (2). Confidence bounds (68%; 1σ) were determined for the fitted coefficients. Data were excluded from further analysis if the ratio between the upper and lower bound of the confidence interval was greater than 10, as these data do not follow a Rouse relation for unknown reasons (for example, measurement error) and would appear as sparse outliers. We also eliminated points with $P_i < 0.01$, as these profiles are nearly vertical, which poorly constrains settling velocity to be very near zero. About 15% of the data were excluded on the basis of these criteria. To calculate the near-bed reference concentration, we used the fitted Rouse profile to extrapolate or interpolate the concentration to a reference level at 10% of the flow depth above the bed, which was found to best collapse the sand data[20].

The Rouse equation (equation (1)) can be derived assuming an equilibrium suspension where the upwards flux of sediment due to turbulence, parameterized using a parabolic vertical eddy viscosity distribution, is balanced by a downwards gravitational settling flux[19,47]. We used the best-fit two-parameter model for β in the Rouse number (equation (2)) that was found for sand suspensions[20]; that is, $\beta_i = 16.82\left(\frac{u_{*\mathrm{sk}}}{w_{\mathrm{si}}}\right)^{-0.54} C_{\mathrm{f}}^{0.3}$. The skin-friction portion of the total shear velocity (minus the portion due to form drag), was calculated using the Manning–Strickler relation[3], $\frac{U}{u_{*\mathrm{sk}}} = 8.1\left(\frac{H_{\mathrm{sk}}}{k_{\mathrm{s}}}\right)^{1/6}$, where $k_{\mathrm{s}} = 3D_{84}$ is the grain roughness on the bed, D_{84} is the 84th percentile of the cumulative size distribution of bed material and H_{sk} is the depth due to skin friction. To calculate the settling velocity of individual particles, we used Ferguson and Church[39], $w_{\mathrm{si}} = \frac{RgD_i^2}{C_1\nu + \left(0.75C_2RgD_i^3\right)^{0.5}}$, in which $R = 1.6$ is the submerged specific density of sediment, ν is the kinematic viscosity of the fluid, and $C_1 = 18$ and $C_2 = 1$ are constants set for natural sediment. The flow resistance coefficient is $C_{\mathrm{f}} = \frac{u_*^2}{U^2}$, where the total shear velocity is $u_* = \sqrt{gHS}$ assuming steady, uniform flow.

To estimate the size of flocs, we used the floc settling velocity model for small settling Reynolds numbers[22,23]

$$w_{\mathrm{s,eff}} = \frac{1}{b_1}\frac{R_{\mathrm{p}}gD_{\mathrm{f}}^{n_{\mathrm{f}}-1}D_{\mathrm{p}}^{3-n_{\mathrm{f}}}}{\nu} \quad (4)$$

where $R_{\mathrm{p}} = 1.6$. We estimated D_{p} as the median particle size for all sizes less than 40 μm (that is, those inferred to be flocculated; Fig. 2c) for each dataset, and set $n_{\mathrm{f}} = 2.5$ and $b_1 = 100$ (ref. [23]). Inserting these parameters into equation (4) and rearranging allowed us to solve for the characteristic floc diameters (Fig. 3). We then calculated the floc submerged specific density from Kranenburg[21] as $R_{\mathrm{f}} = R_{\mathrm{p}}(D_{\mathrm{f}}/D_{\mathrm{p}})^{n_{\mathrm{f}}-3}$ (Fig. 3).

Data availability

All data used in the study are previously published (Extended Data Table 1) and available in de Leeuw et al.[20].

References

40. Jordan, P. R. *Fluvial Sediment of the Mississippi River at St. Louis, Missouri* Water Supply Paper No. 1802 (USGS, 1965); https://doi.org/10.3133/wsp180
41. Nittrouer, J. A., Mohrig, D., Allison, M. A. & Peyret, A.-P. B. The lowermost Mississippi River: a mixed bedrock-alluvial channel. *Sedimentology* **58**, 1914–1934 (2011).
42. Colby, B. R. & Hembree, C. H. *Computations of Total Sediment Discharge, Niobrara River near Cody, Nebraska* Water Supply Paper No. 1357 (USGS, 1955); https://doi.org/10.3133/wsp1357
43. Nordin, C. F. & Dempster, G. R. *Vertical Distribution of Velocity and Suspended Sediment, Middle Rio Grande, New Mexico* (USGS, 1963).
44. Hubbell, D. W. & Matejka, D. Q. *Investigations of Sediment Transportation, Middle Loup River at Dunning, Nebraska: With Application of Data from Turbulence Flume* Water Supply Paper No.1476 (USGS, 1959); https://doi.org/10.3133/wsp1476
45. Haught, D., Venditti, J. G. & Wright, S. A. Calculation of in situ acoustic sediment attenuation using off-the-shelf horizontal ADCPs in low concentration settings. *Water Resour. Res.* **53**, 5017–5037 (2017).
46. Moodie, A. J. Yellow River Kenli Lijin Station Survey. *Zenodo* https://doi.org/10.5281/zenodo.3457639 (2019).
47. Vanoni, V. A. Transportation of suspended sediment by water. *Trans. Am. Soc. Civ. Eng.* **111**, 67–102 (1946).

Acknowledgements

This research was sponsored by a National Science Foundation grant (number EAR 1427262) to M.P.L., J.A.N. and G.P., and a Caltech Discovery grant to M.P.L. and W.W.F.

Author contributions

M.P.L., W.W.F. and G.P. designed the study. M.P.L. and J.d.L. analysed data. A.J.M., J.G.V., J.A.N. and D.H. contributed data. M.P.L. led the writing of the manuscript with contributions from all authors.

Competing interests

The authors declare no competing interests.

Additional information

Extended data is available for this paper at https://doi.org/10.1038/s41561-020-0602-5.

Correspondence and requests for materials should be addressed to M.P.L.

Peer review information Primary Handling Editor: Tamara Goldin.

Reprints and permissions information is available at www.nature.com/reprints.

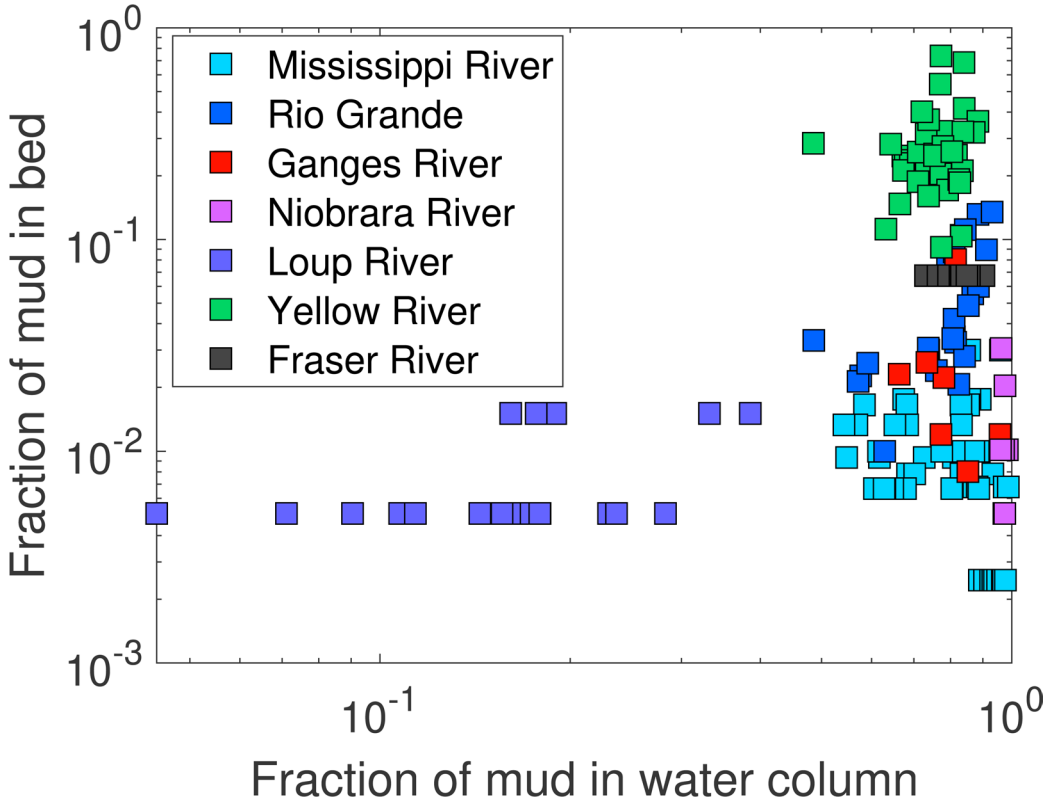

Extended Data Fig. 1 | Mud abundances in sand-bedded rivers. Fraction of mud measured in the bed material and that measured from the total suspended sediment in the water column when depth averaged from the field data in our database (Table S1). Except for the Loup River, mud typically constitutes > 70% of the suspended sediment, but generally < 10% of the bed material (with the exception of the Yellow River).

Data source	Location	Median bed material grainsize, D_{50} (μm)	Water depth, H (m)	Number of grainsize classes	Number of profiles
Jordan [1965]	Mississippi at St Louis	189-457	3.54-16.34	12	51
Nitrouer et al. [2011]	Mississippi at Empire reach	166-244	12.96-32.38	43	9
Lupker et al. [2011]	Ganges at Harding bridge	159-268	10.0-14.0	31	7
Nordin & Dempster [1963]	Rio Grande	166-439	0.2-0.78	12	23
Moodie [2019]	Yellow River	44-112	1.55-7.65	51	35
Haught et al. [2017]	Fraser River	300	8.7-14.5	60	25
Hubbell & Matejka [1959]	Middle Loup River	313-517	0.33-1.19	10	20
Colby & Hembree [1955]	Niobrara River	226-305	0.24-0.7	7	10

Extended Data Table 1 | Data sources. Suspended sediment concentration profiles used in our analyses[38-45].